Design of Enzyme

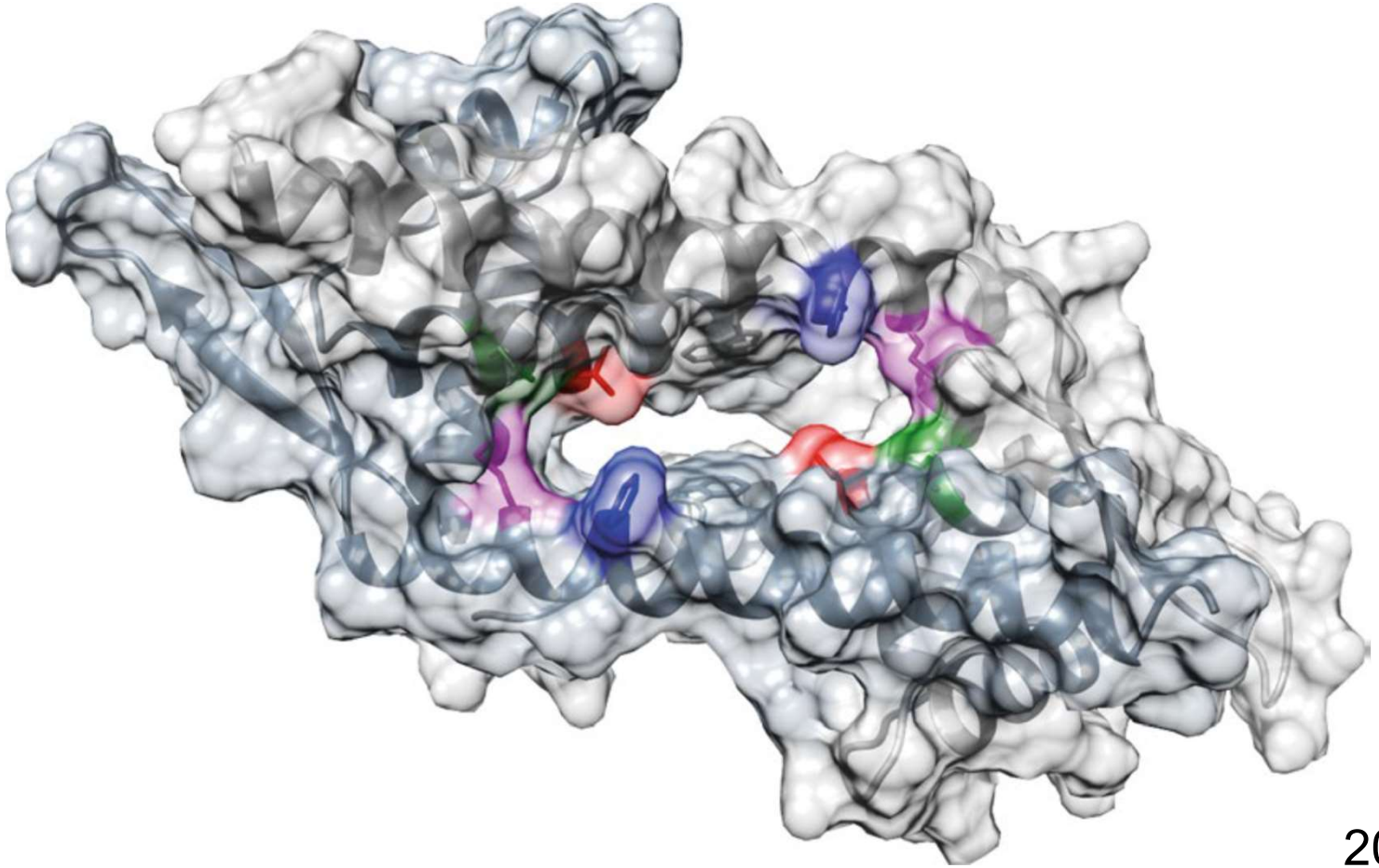

20180714
Literature Seminar
Yun-wei Xue

Contents

1. Introduction
2. De novo design
3. Incorporation of unnatural amino acid (main paper)

1.1 Advantages and limitations of natural enzyme

[1]

Advantages	Limitations	
1. Enviable efficiency	1. Not optimal for abiological tasks	← section 2
2. Enviable selectivity	2. A narrow substrate range	← section 3 (main paper)
	3. Difficult to produce	
	4. Lack appropriate stability	

1. Hilvert, D. *Annu. Rev. Biochem.* **2013**, *82*, 447.

1.2 Concepts and methods of enzyme design

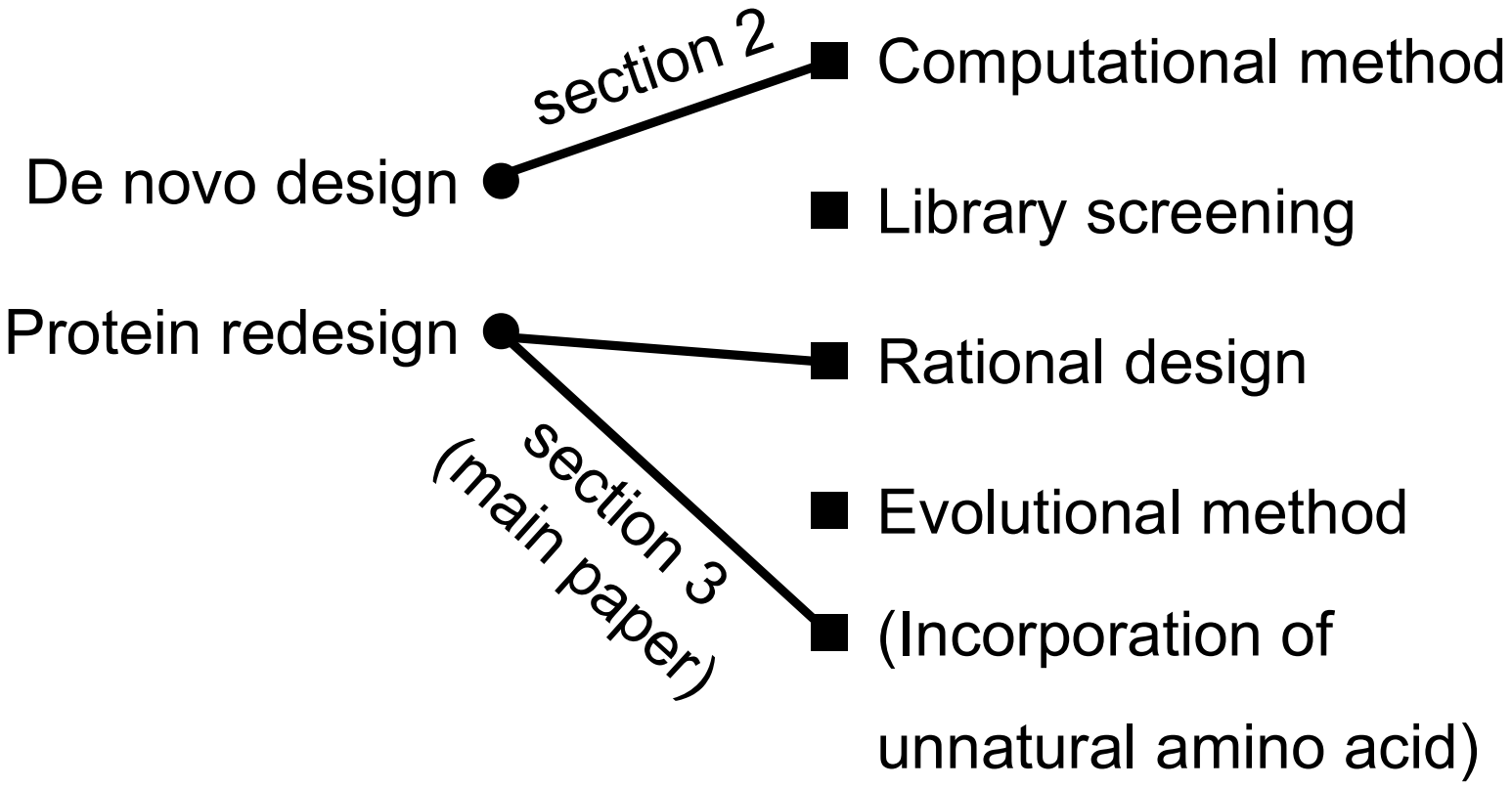

Contents

1. Introduction

2. De novo design

REPORT

Computational Design of an Enzyme Catalyst for a Stereoselective Bimolecular Diels-Alder Reaction

Justin B. Siegel[1,2,*], Alexandre Zanghellini[1,2,*,†], Helena M. Lovick[3], Gert Kiss[4], Abigail R. Lambert[5], Jennifer L. St.Clair[1]...
+ See all authors and affiliations

Science 16 Jul 2010:
Vol. 329, Issue 5989, pp. 309-313
DOI: 10.1126/science.1190239

2.1 Procedure of de novo design through computational method

Step 1. Decision of catalytic mechanism and an associated ideal active site (**10^{19}** possible configurations)

Step 2. Design of enzyme models (theozyme + protein scaffold) (**10^{6}** designs)

filtration based on various parameters

Step 3. Experimental validation (**84** designs)

filtration based on experimental validation

Step 4. Further improvement (**2** designs)

1. Baker, D. *et al*. *Science* **2010**, *329*, 309.

2.2 Catalytic mechanism

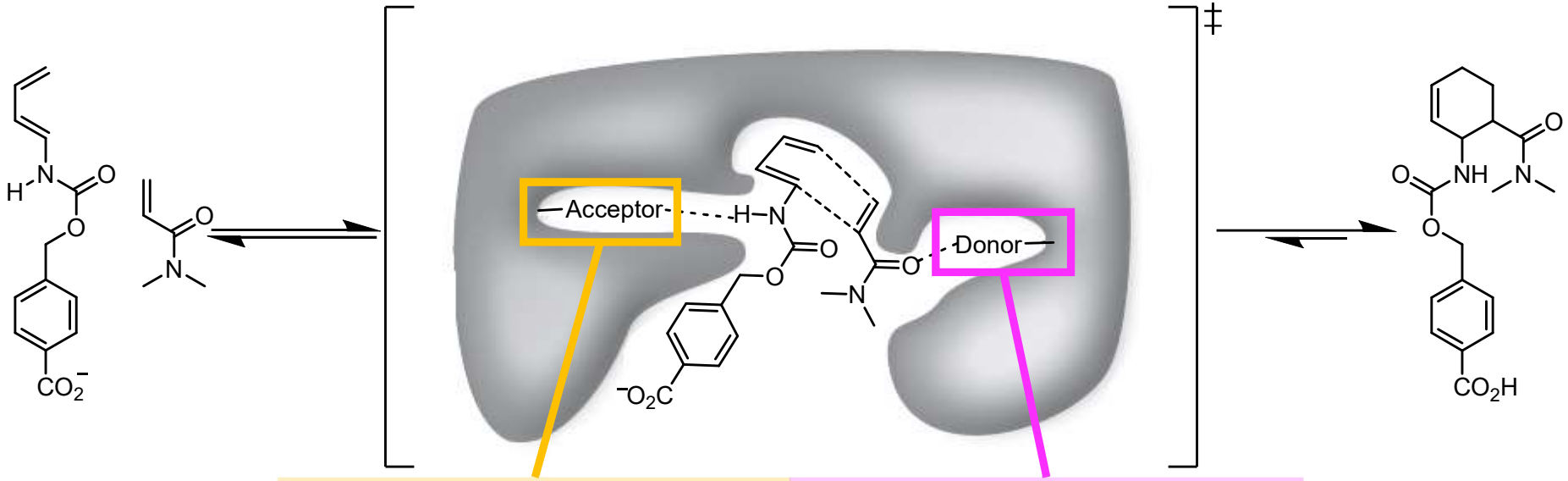

Raising HOMO energy & stabilizing the positive charge accumulating in TS

Lowing LUMO energy & stabilizing the negative charge accumulating in TS

Narrowing the energy gap between HOMO and LUMO, stabilizing the TS, thus increasing the rate

1. Baker, D. *et al*. *Science* **2010**, *329*, 309.
2. Jorgensen, W. L.*J. Org. Chem.***1994**, *59*, 803.

2.3 Design of enzyme models

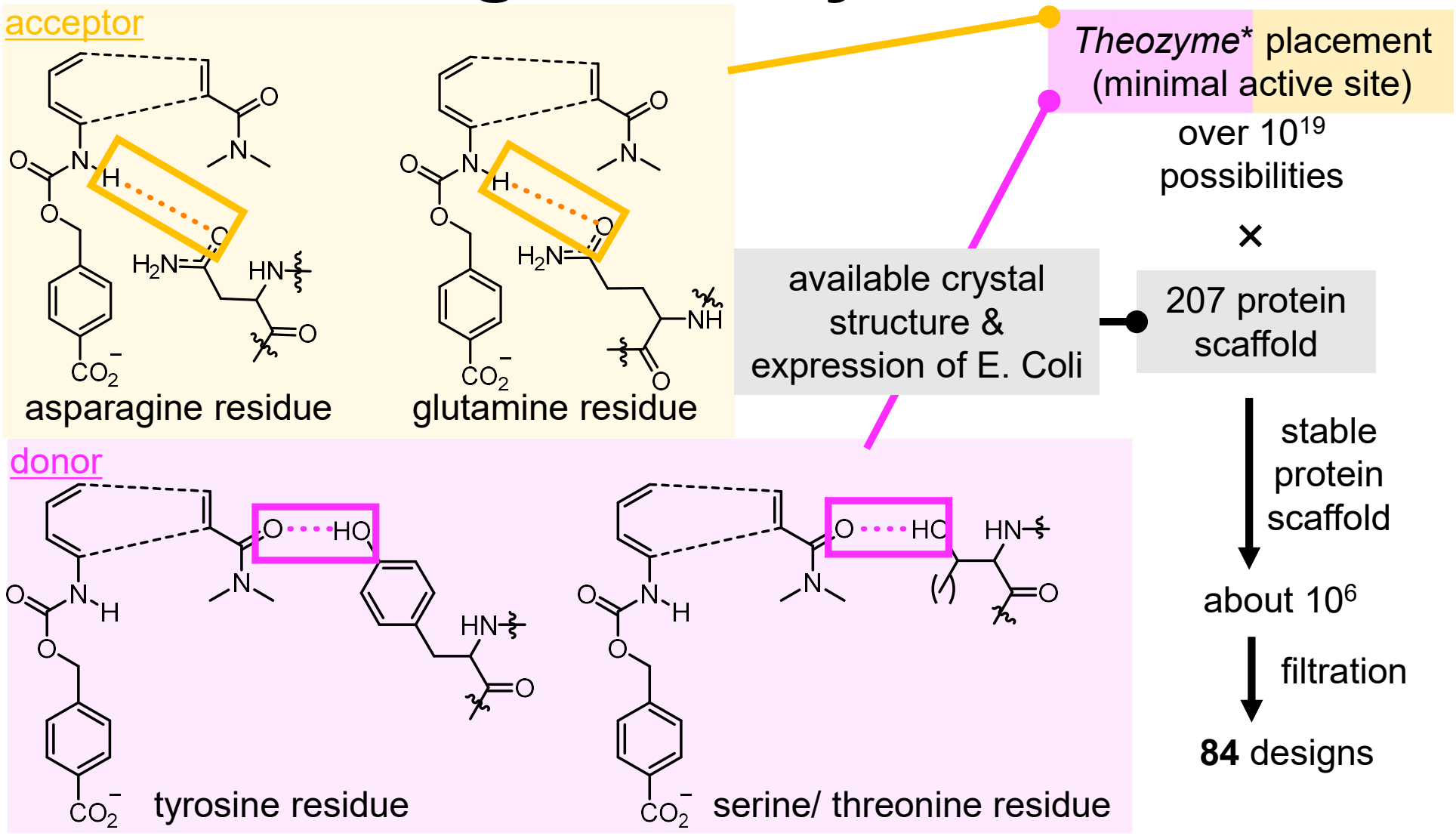

1. Baker, D. *et al*. *Science* **2010**, *329*, 309.
2. Baker, D. *et al*. *Pro. Sci.* **2006**, *15*, 2785.

2.4 Experimental validation

84 designs

expression in *E. Coli*

50 designs (soluble)

D-A product formation assay (by LC-MS)

2 designs (Diels-Alderase active)

DA_20_00 **DA_42_00**

DA_20_00

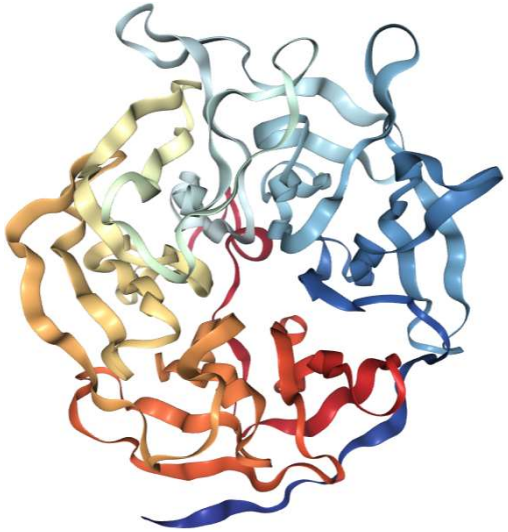

- derived from a six-bladed β-propeller scaffold (PDB ID: 1E1A) (13 mutations)

DA_42_00

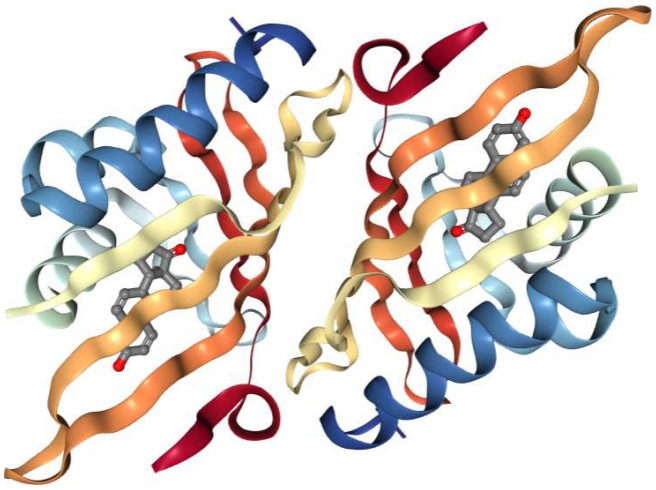

- derived from the ketosteroid isomerase scaffold (PDB ID: 1OHO) (14 mutations)

1. Baker, D. *et al*. *Science* **2010**, *329*, 309.

2.5 Further optimization

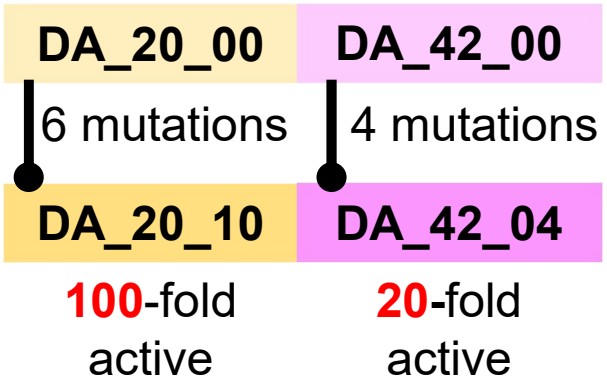

Catalyst	k_{cat} (hour^{-1})	$K_{M\text{-diene}}$ (mM)	$K_{M\text{-dienophile}}$ (mM)	$k_{cat}/K_{M\text{-diene}}$ (s^{-1} M^{-1})	$k_{cat}/K_{M\text{-dienophile}}$ (s^{-1} M^{-1})	$k_{cat}/(K_{M\text{-diene}} \times K_{M\text{-dienophile}})$ (s^{-1} M^{-1} M^{-1})
DA_20_00	0.10 ± 0.02	3.5 ± 1.5	146.0 ± 2.5	0.008	0.0002	0.06
DA_20_10	2.13 ± 0.24	1.3 ± 0.1	72.8 ± 5.1	0.455	0.0081	6.23
DA_42_04	0.03 ± 0.01	0.5 ± 0.1	16.2 ± 3.2	0.017	0.0005	1.03
mAb 7D4	0.21	1.0	1.7	0.058	0.0343	20.18
mAb 4D5	0.21	1.6	5.9	0.036	0.0099	6.19

Table 1. Kinetic parameters for DA_20_00, DA_20_10, and DA_42_04.

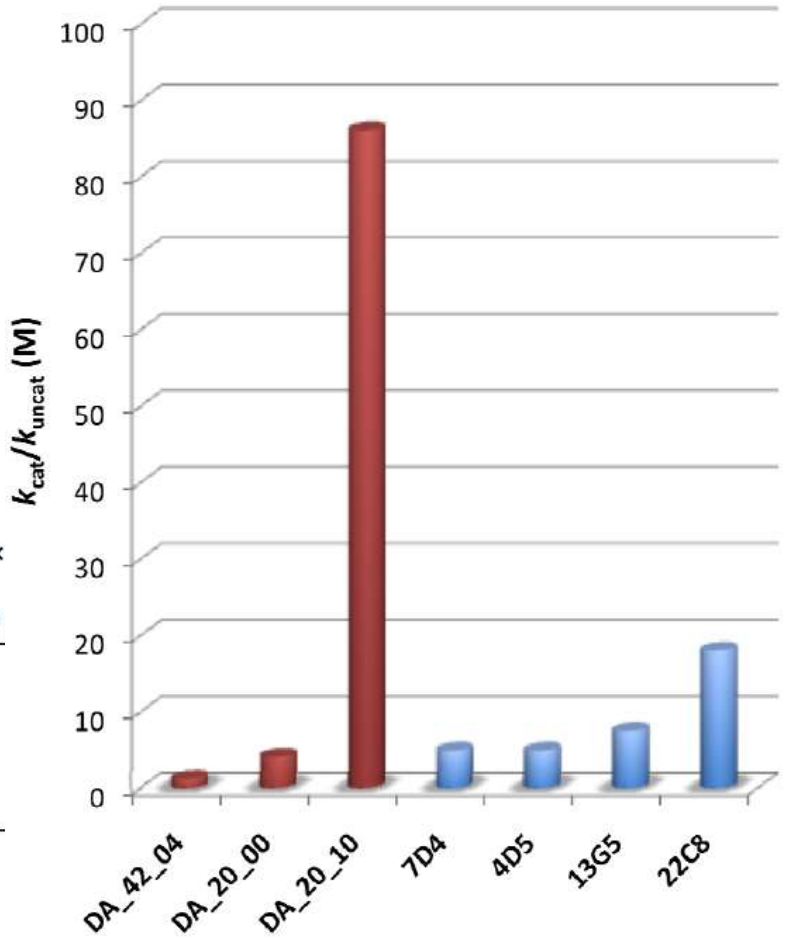

Figure 1. Effective molarity of DA_20_00, DA_20_10, and DA_42_04 compared to catalytic antibodies.

1. Baker, D. *et al*. *Science* **2010**, *329*, 309.
2. Janda, K. D. *J. et al*. *Am. Chem. Soc.* **1995**, *117*, 7041.

2.6 Stereoselectivity

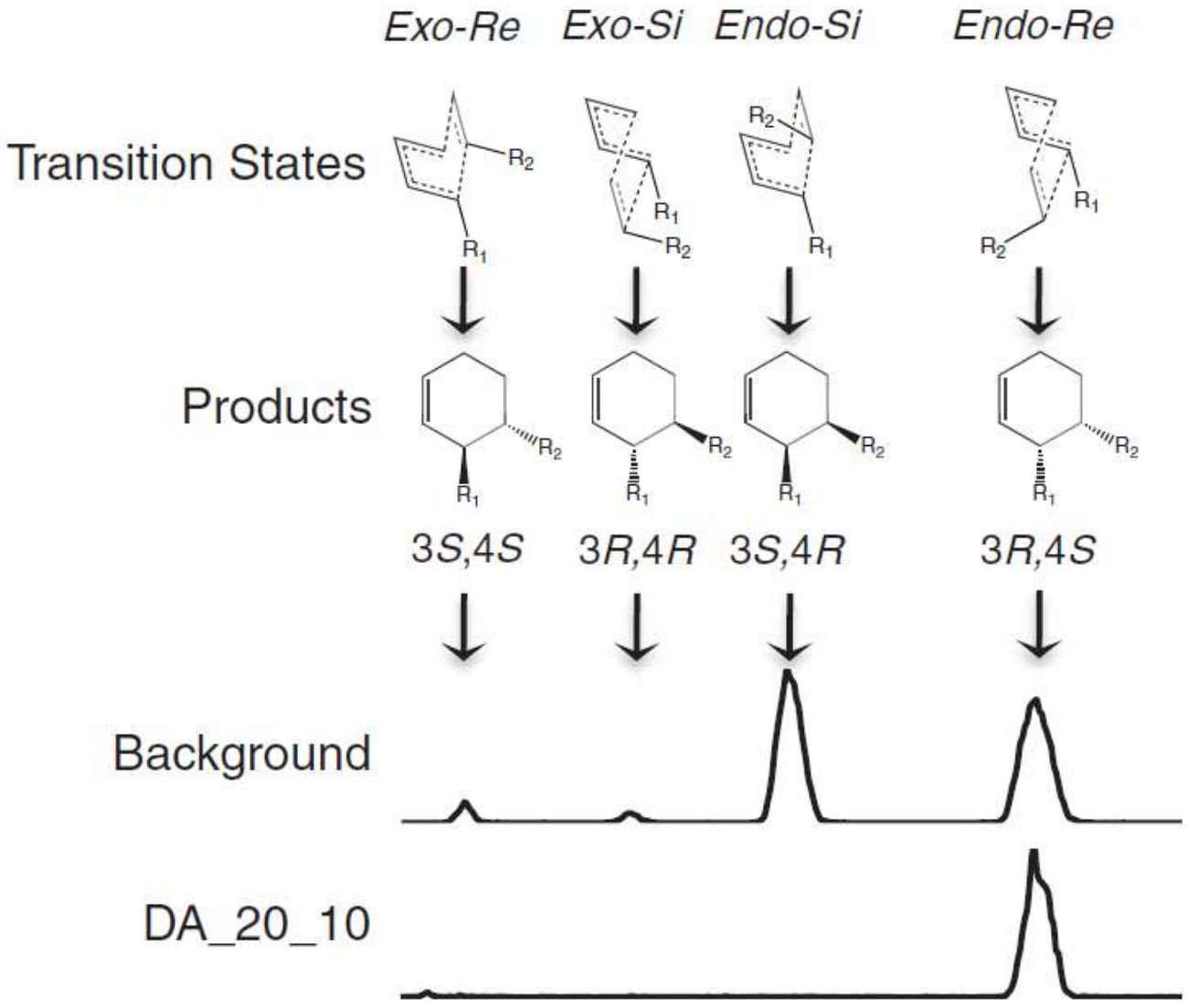

Figure 2. Stereoselectivity of DA_20_10.

1. Baker, D. *et al*. *Science* **2010**, *329*, 309.

2.7 Substrate specificity

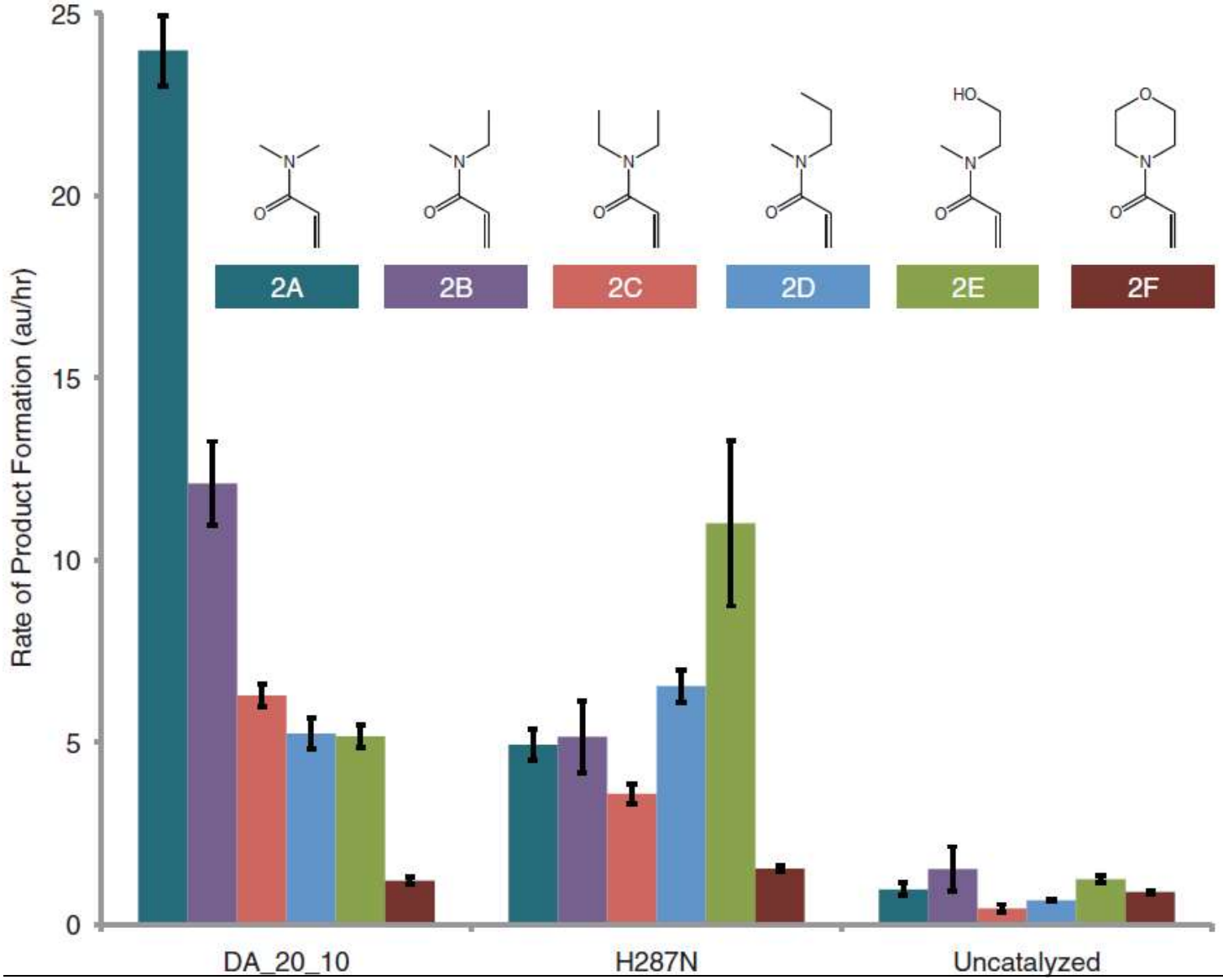

Figure 3. Control of substrate specificity.

1. Baker, D. *et al*. *Science* **2010**, *329*, 309.

2.8 Short summary

Mechanism

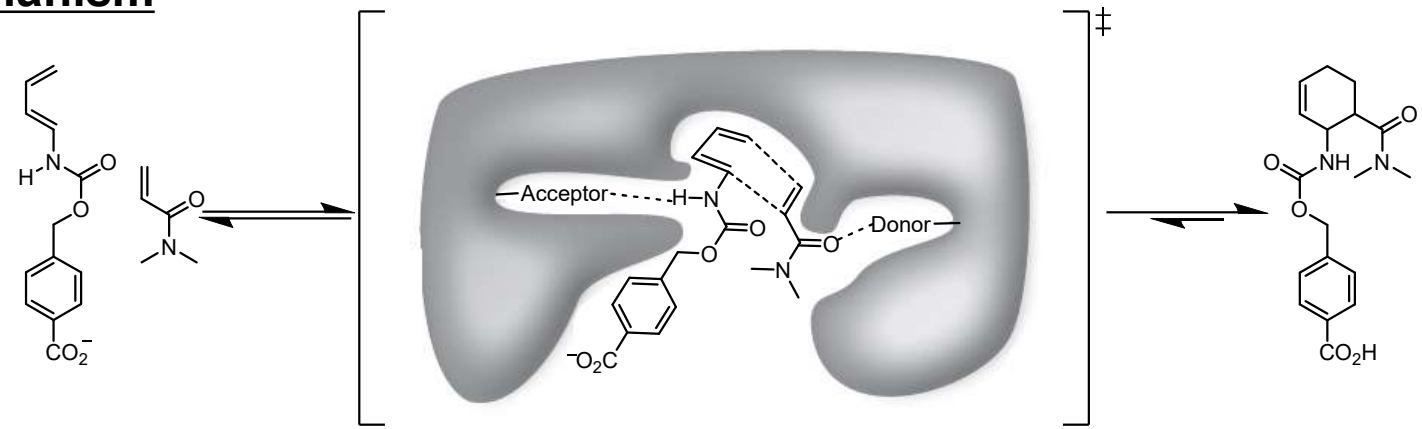

Design

acceptor

donor

Theozyme × protein scaffold

Method

computational assistance → *experimental validation*

2 active designs

→ *optimization*

artificial enzyme with **high efficiency** and **selectivity** for bimolecular Diels-Alder reaction

abiological task

Improvements needed

- low hit probability (2 out 50 proved to be active)
- limited applicable functions
- effort-consuming process

1. Baker, D. *et al*. *Science* **2010**, *329*, 309.

Contents

1. Introduction
2. De novo design
3. Incorporation of unnatural amino acid (main paper)

A designer enzyme for hydrazone and oxime formation featuring an unnatural catalytic aniline residue

Ivana Drienovská, Clemens Mayer, Christopher Dulson and Gerard Roelfes*

Gerard Roelfes

2000 M.Sc. and Ph. D.
University of Groningen, the Netherlands
(Prof. Ben L. Feringa, on synthetic models for enzyme)

2000-2003 Post-doc. fellow
Laboratory for organic chemistry of ETH-Zürich (Switzerland)
(Prof. Donald Hilvert, on synthetic strategy towards seleno-proteins)

2003-2006 Junior research group leader
University of Groningen

2006-2010 Assistant professor

2010-2015 Associate professor

2015- Full professor of biomolecular chemistry and catalysis

Research interests:

- *DNA based catalysis*
- ***Artificial enzymes***
- *Bioorthogonal metal catalysis*
- *Artificial allosteric systems*
- *Targeting of ROS in living cells*

3.1 Protein template for redesign

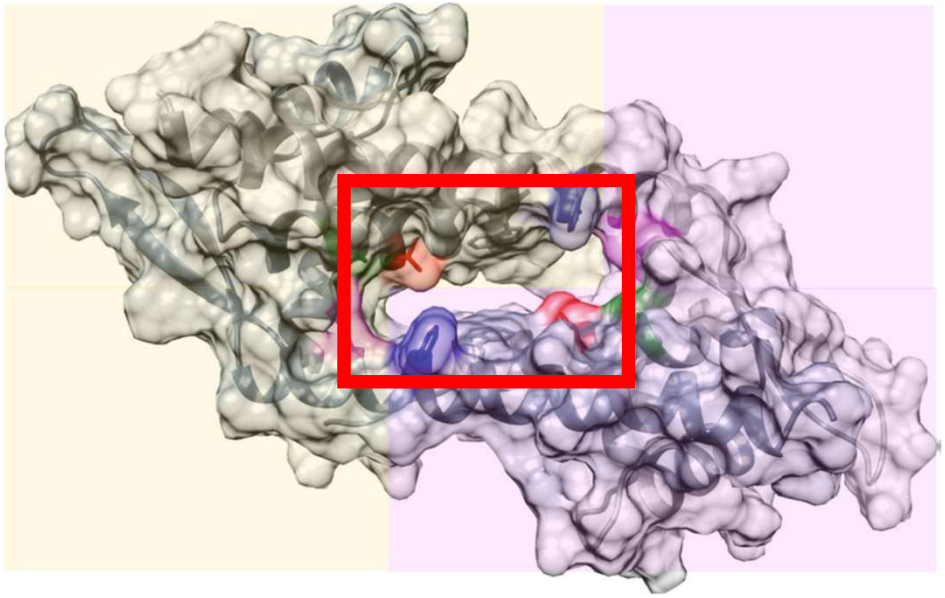

Figure 4. Surface view of the dimeric LmrR (PDB ID: 4ZZD)

- homodimeric protein
- 13,5 kDa per monomer
- an unusual large hydrophobic pore at the dimer surface (as depicted in red frame)

Previous work based on this protein:

- **Diels-Alder reaction**

Roelfes, G. *et al*. *Angew. Chem., Int. Ed.* **2012**, *51*, 7472.

- **Hydration**

Roelfes, G. *et al*. *Chem. Sci.* **2013**, *4*, 3578.

- **Friedel-Crafts alkylation reaction**

Roelfes, G. *et al*. *Chem. Sci.* **2015**, *6*, 770.
Roelfes, G. *et al*. *J. Am. Chem. Soc.* **2015**, *137*, 9796.

Main paper:

- **Hydrazone and oxime formation**

nature chemistry ARTICLES
https://doi.org/10.1038/s41557-018-0082-z

A designer enzyme for hydrazone and oxime formation featuring an unnatural catalytic aniline residue

Ivana Drienovská, Clemens Mayer, Christopher Dulson and Gerard Roelfes*

1. Shimada, I. *et al*.*Sci. Rep.***2014**, *4*, 6922.
2. Thunnissen, A. *et al*. *EMBO J.* **2008**, *28*, 156.

3.2 Enzyme design

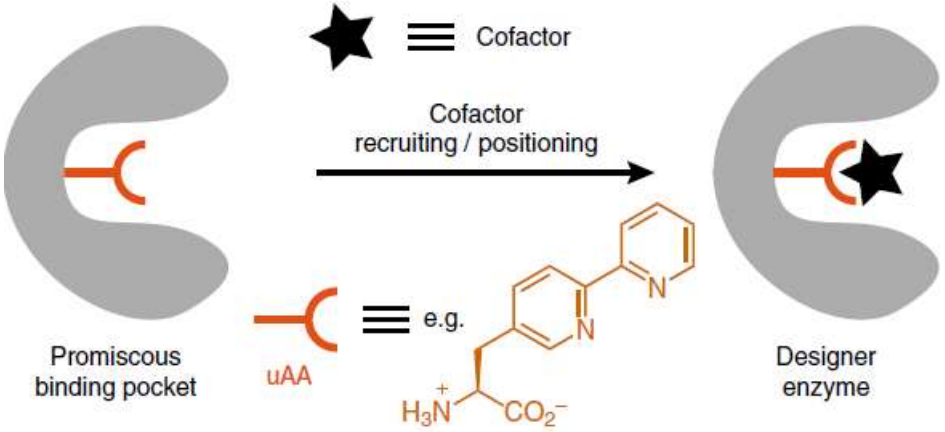

In previous work, catalysis was achieved through incorporation of metal-binding **unnatural amino acids** where they do **not** actively participate in catalysis but work as a kind of **cofactor recruiter**.

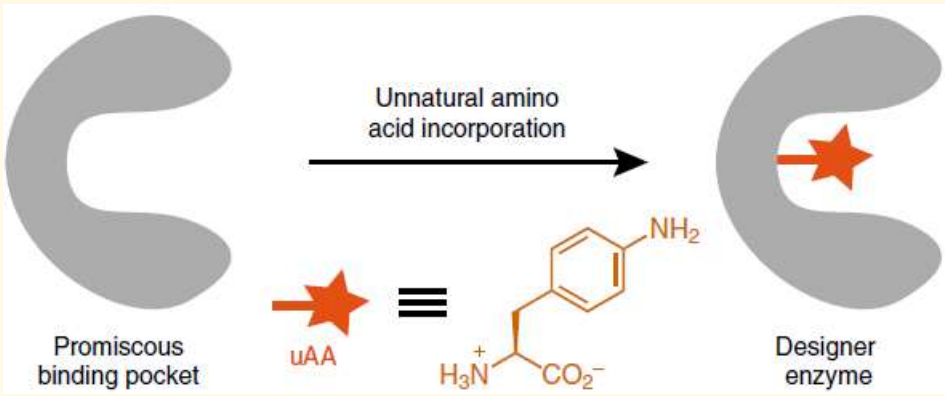

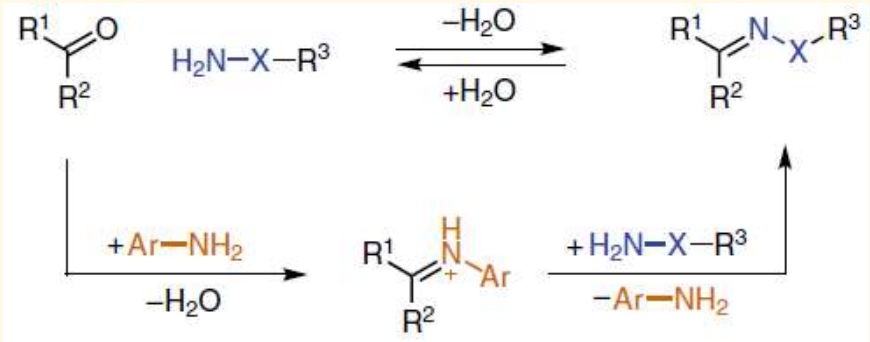

hydrazone (X = NH), oxime (X = O).

In this work, **unnatural amino acid (pAF, *p*-aminophenylalanine)** is inserted to act as catalytic residue to catalyze hydrazone and oxime formation.

1. Roelfes, G. *et al*. *Chem. Sci.* **2015**, *6*, 770.
2. Jencks, W. P. *et al*. *J. Am. Chem. Soc.***1962**, *84*, 826.

3.2 Enzyme design

Positions selected for incorporation of pAF

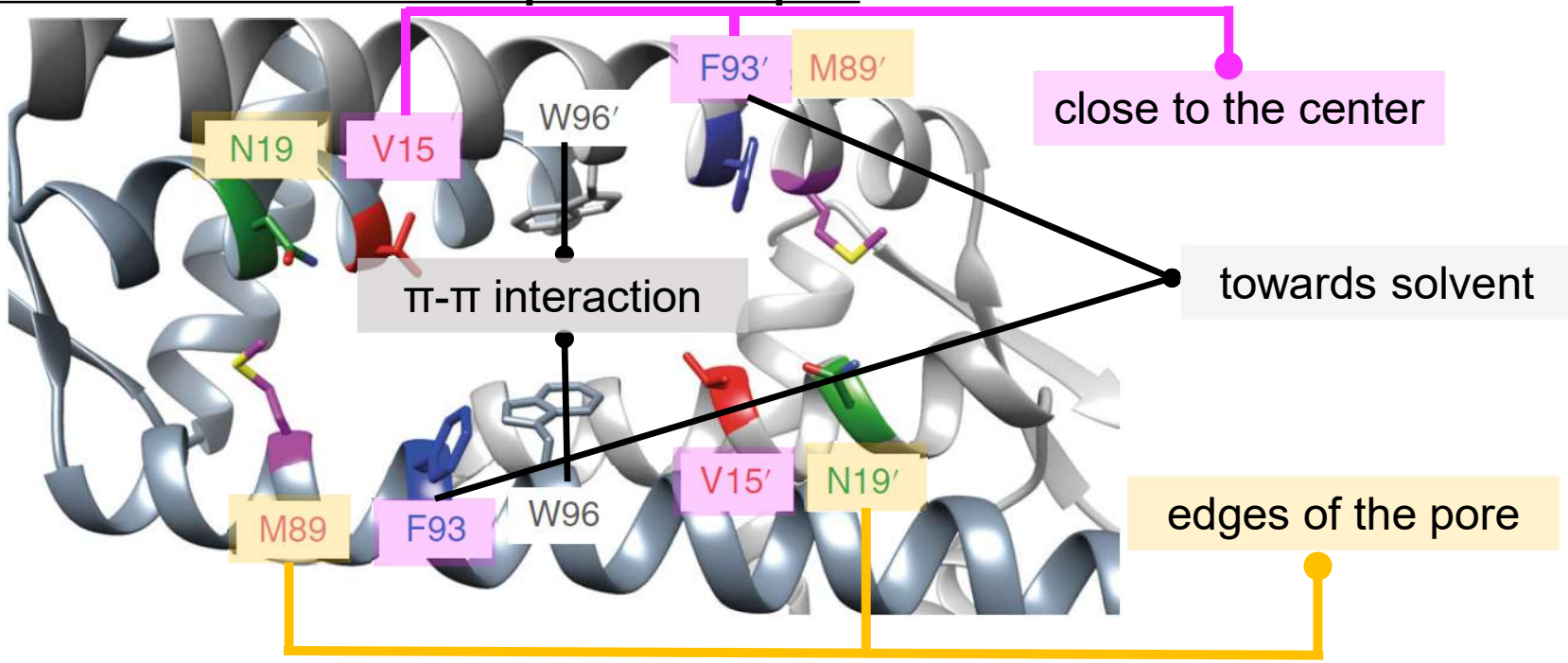

LmrR variants preparation

Introduction of *p*-azidophenylalanine (pAzF) through *E. Coli* expression → Subsequent reduction with tris(2-carboxyethyl)phosphine (TCEP) → desired **LmrR variants**

1. Roelfes, G. *et al*. *Nat. Chem.*, 2018, AOP.

3.3 Hydrazone formation

Model reaction for evaluating the catalytic potential

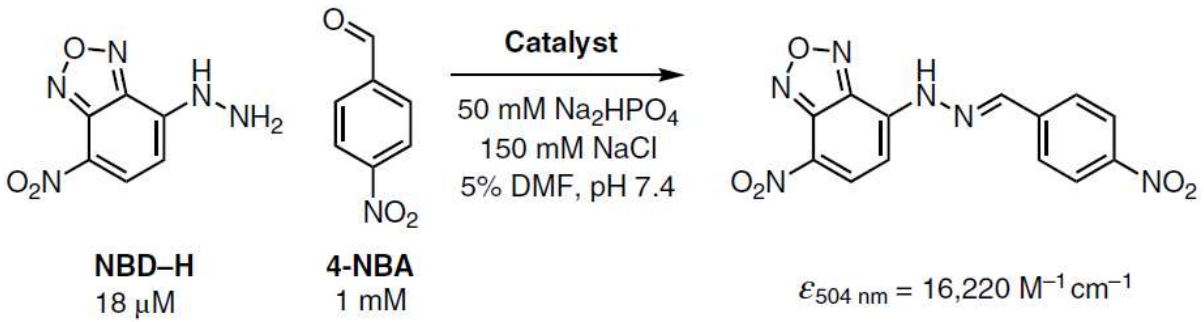

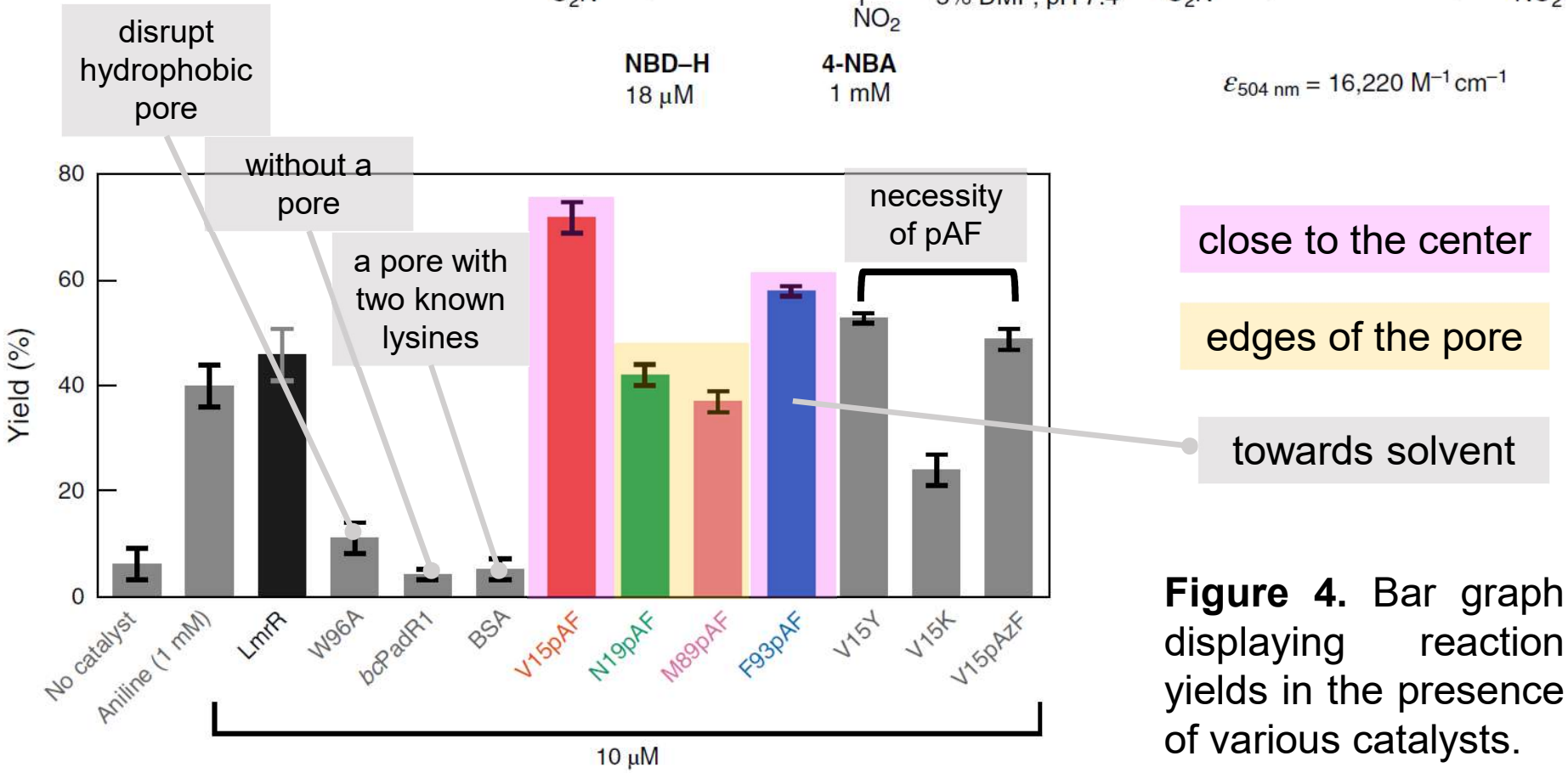

Figure 4. Bar graph displaying reaction yields in the presence of various catalysts.

1. Roelfes, G. *et al*. *Nat. Chem.*, 2018, AOP.

3.4 Intermediate analysis

Mechanism

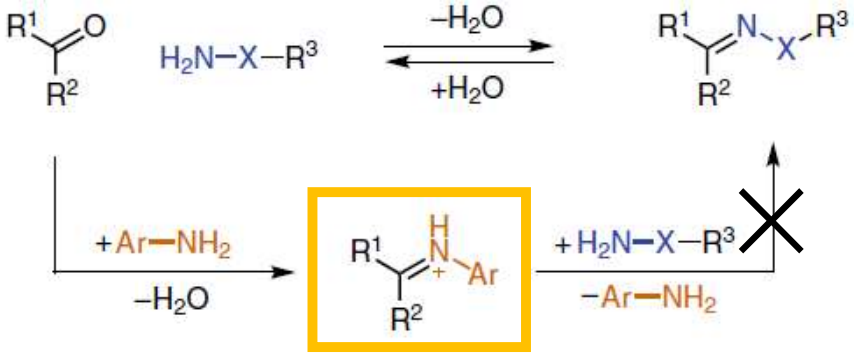

Analysis method

LmrR

LmrR_V15pAF

+

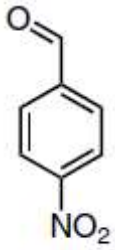

4-NBA

Schiff base intermediate

$NaCNBH_3$ reduction

modified LmrR variants → high-resolution mass spectrometry

Analysis result

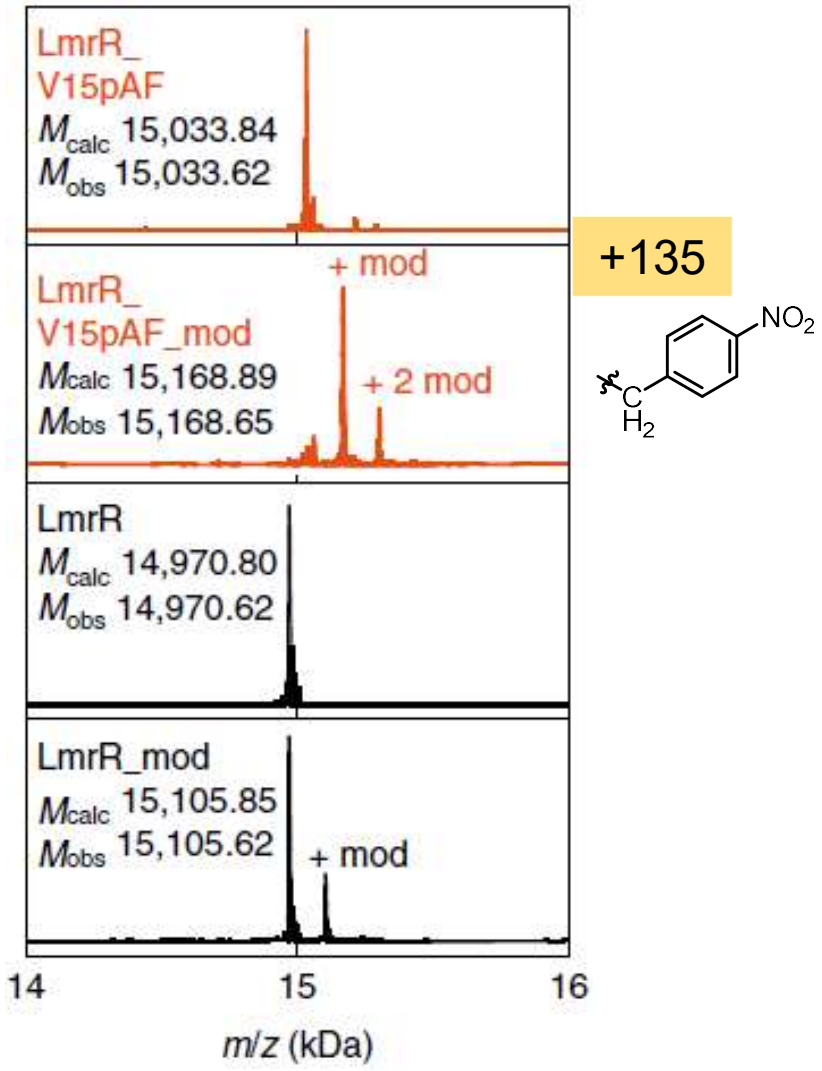

+135

1. Roelfes, G. *et al*. *Nat. Chem.*, 2018, AOP.

3.4 Intermediate analysis

Analysis method

modified LmrR variants → tryptic digestion → resulting peptides → LC-MS/ high-resolution MS analysis

Analysis result

LC-MS

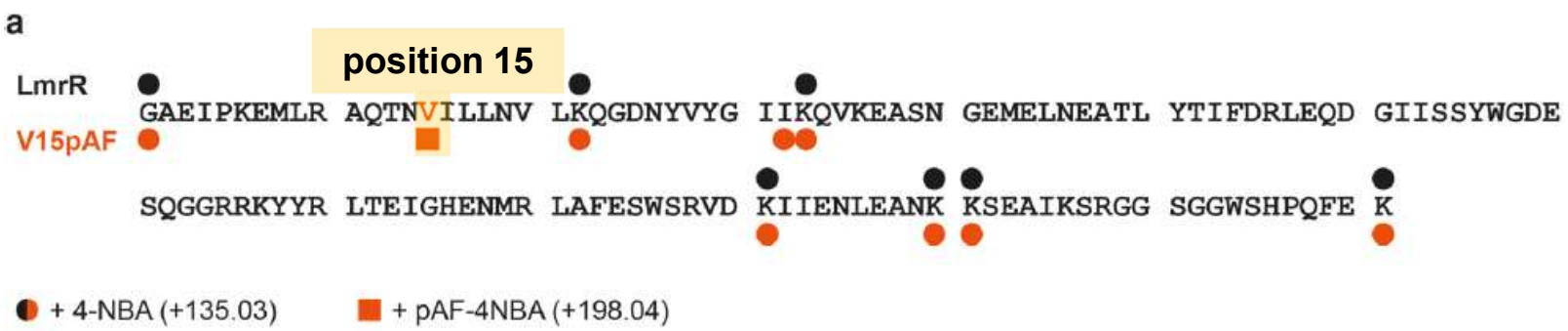

high-resolution MS

b

peptide	mass (Da)	ppm
AQTNVILLNVLK	1324.808	0.2
AQTNVILLNVLK (+198.04)	1522.851	3.9
AQTNVILLNVLKQGDNYVYGIIK	2575.437	-0.4
AQTNVILLNVLKQGDNYVYGIIK (+198.04)	2773.480	1.4
AQTNVILLNVLKQGDNYVYGIIKQVK	2930.659	0.9
AQTNVILLNVLKQGDNYVYGIIKQVK (+198.04)	3128.702	0.8

1. Roelfes, G. *et al*. *Nat. Chem.*, 2018, AOP.

3.5 Kinetic characterization

Model reaction for kinetic characterization of LmrR_V15pAF

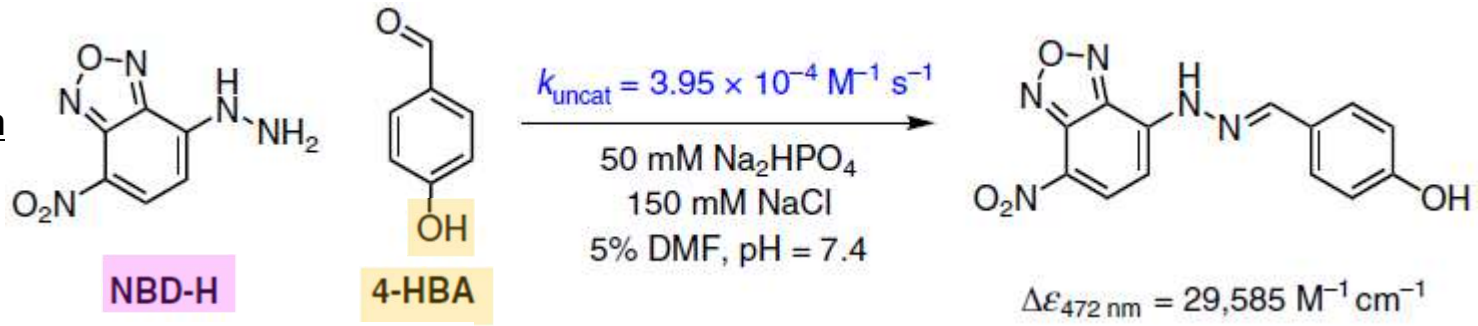

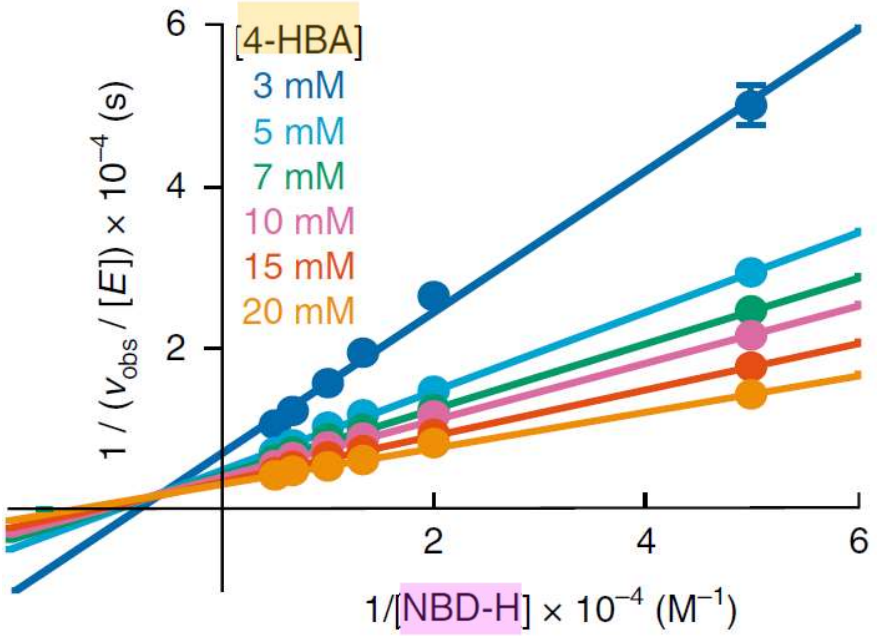

Figure 5. Double-reciprocal plot displaying the dependence of reaction velocity on NBD-H conc. at different 4-HBA conc.

entry	catalyst	rate constant (M^{-2} s^{-1})
1	LmrR_V15pAF	629
2	aniline	1.12

entry	enzyme	k_{uncat} (M^{-1} s^{-1})	k_{cat} (s^{-1})	K_{M1} (M)	K_{M2} (M)	k_{cat} / K_{M1} K_{M2} (M^{-2} s^{-1})	EM (M)	1/TS x 10^{-6} (M^{-1})
1	V15pAF	3.95 x 10^{-4}	5.00 x 10^{-4}	1.00 x 10^{-4}	7.92 x 10^{-3}	6.29 x 10^{2}	1.27	1.6

1. Roelfes, G. *et al*. *Nat. Chem.*, 2018, AOP.

3.5 Kinetic characterization

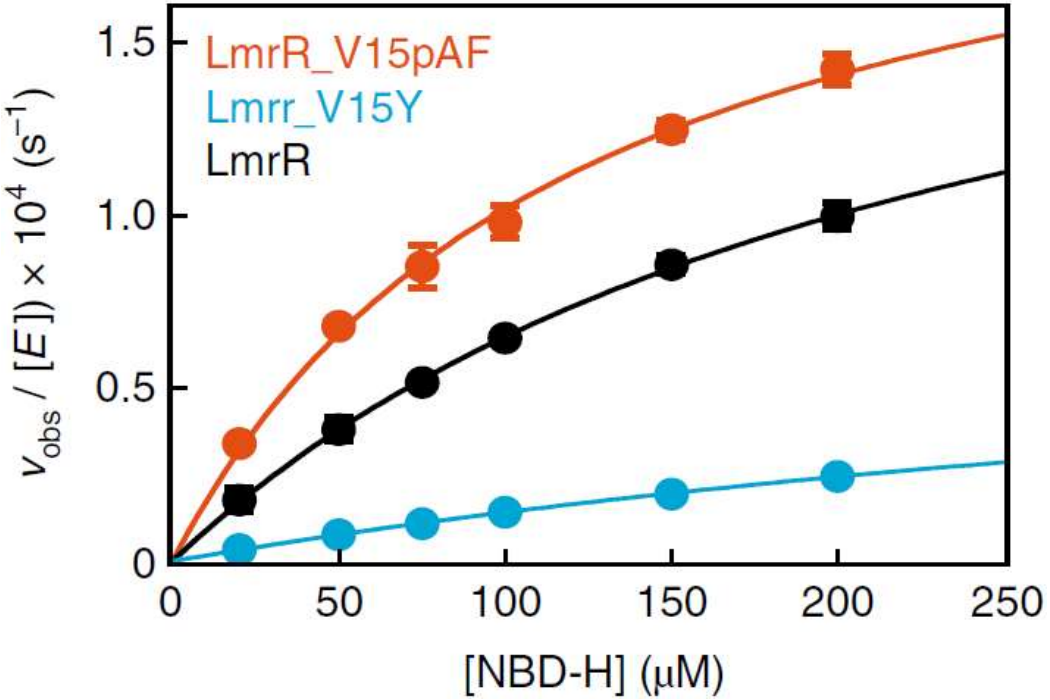

Figure 6. Comparison between the initial reaction rates of LmrR_V15pAF, LmrR_V15Y and LmrR at a 4-HBA conc. of 5 mM.

1. Roelfes, G. *et al*. *Nat. Chem.*, 2018, AOP.

3.6 Oxime formation

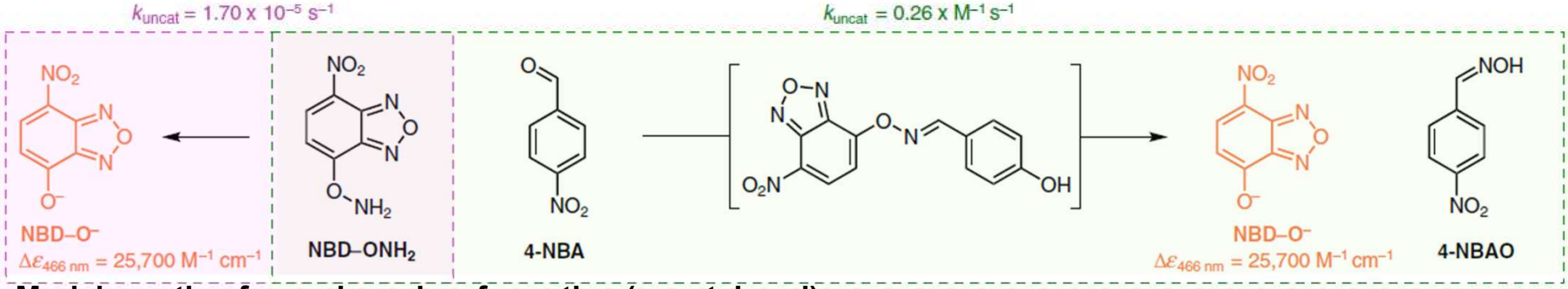

Model reaction for probe oxime formation (uncatalyzed)

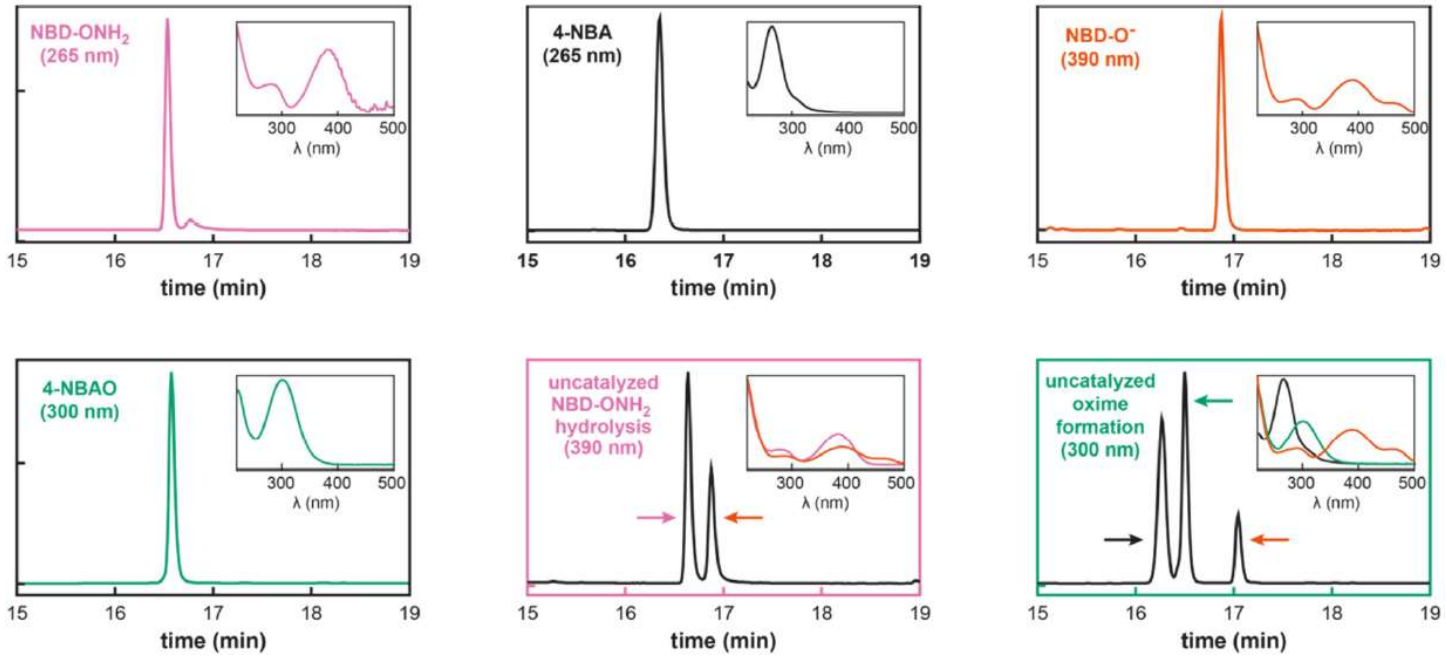

Figure 7. HPLC study for the oxime formation.

1. Roelfes, G. *et al*. *Nat. Chem.*, 2018, AOP.

3.6 Oxime formation

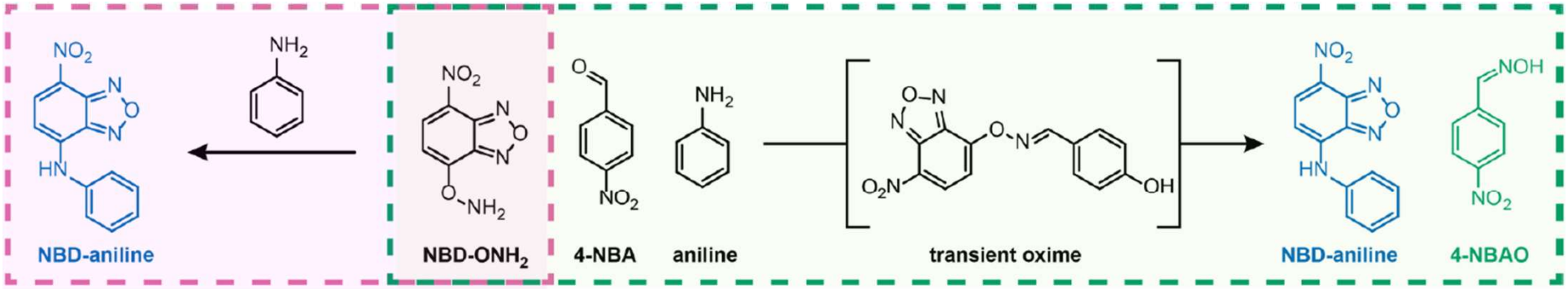

Model reaction for probe oxime formation (catalyzed by aniline)

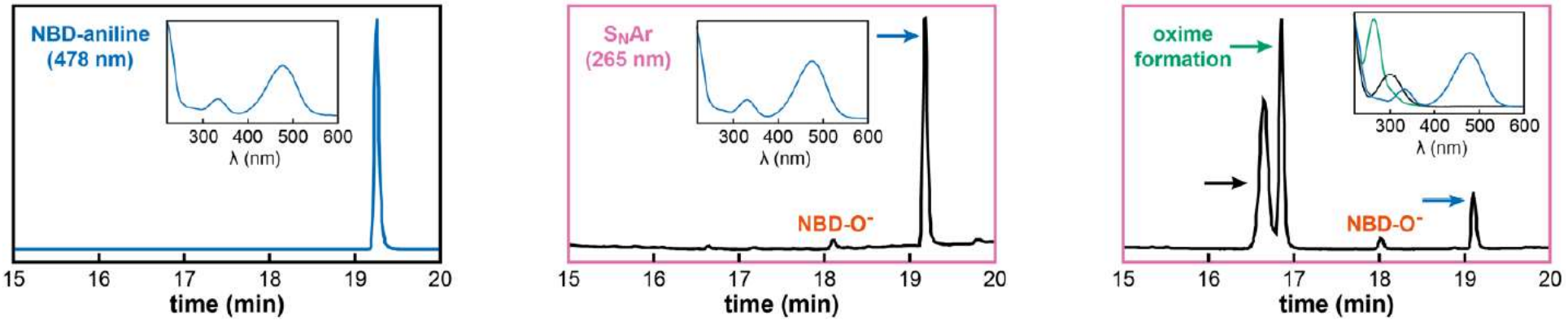

Figure 8. HPLC study for the oxime formation catalyzed by aniline.

1. Roelfes, G. *et al*. *Nat. Chem.*, 2018, AOP.

3.6 Oxime formation

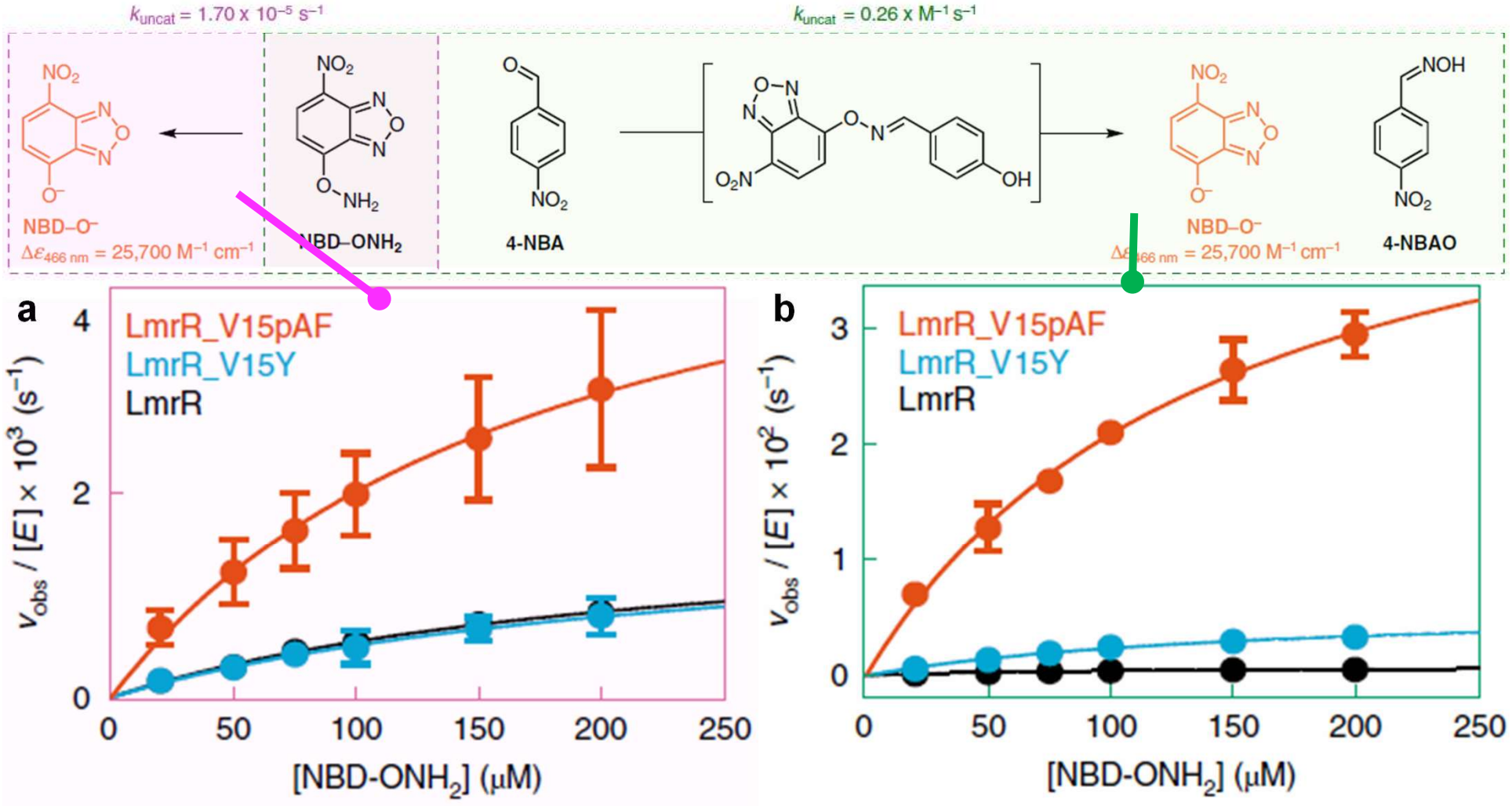

Figure 9. Comparison of initial reaction velocities of LmrR, LmrR_V15Y and LmrR_V15Y for the hydrolysis (**a**) and oxime formation (**b**).

1. Roelfes, G. *et al*. *Nat. Chem.*, 2018, AOP.

3.7 Short summary

Mechanism

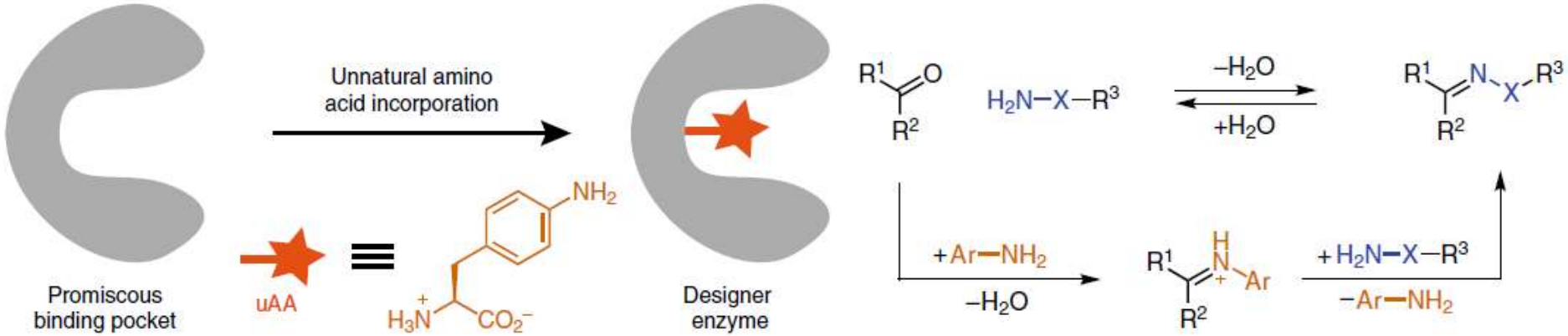

Design

binding pocket of LmrR

Placing of pAF inside the pore → confirmed catalytic reactivity for hydrazone/ oxime formation

Method

Kinetic characterization LC-MS confirmation → designer enzyme derived from a known protein (LmrR) combined with unnatural amino acid for hydrazone/ oxime formation → **broadened substrate range**

Improvements needed

- Not that high efficient (optimization may be necessary)
- Other unnatural amino acid can be screened or designed

1. Roelfes, G. *et al*. *Nat. Chem.*, 2018, AOP.

Summary

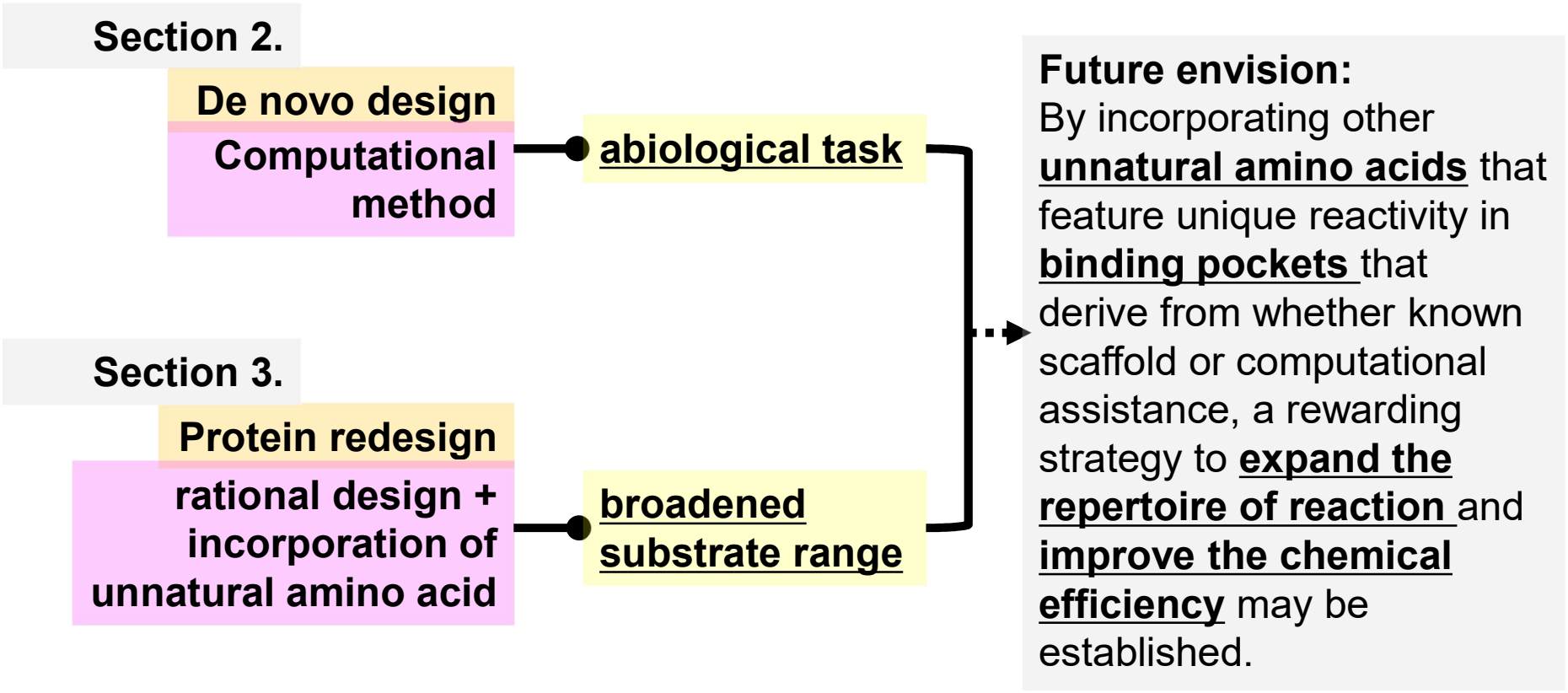

1. Roelfes, G. *et al*. *Nat. Chem.*, 2018, AOP.
2. Baker, D. *et al*. *Science* **2010**, *329*, 309.

Appendix. View of design model

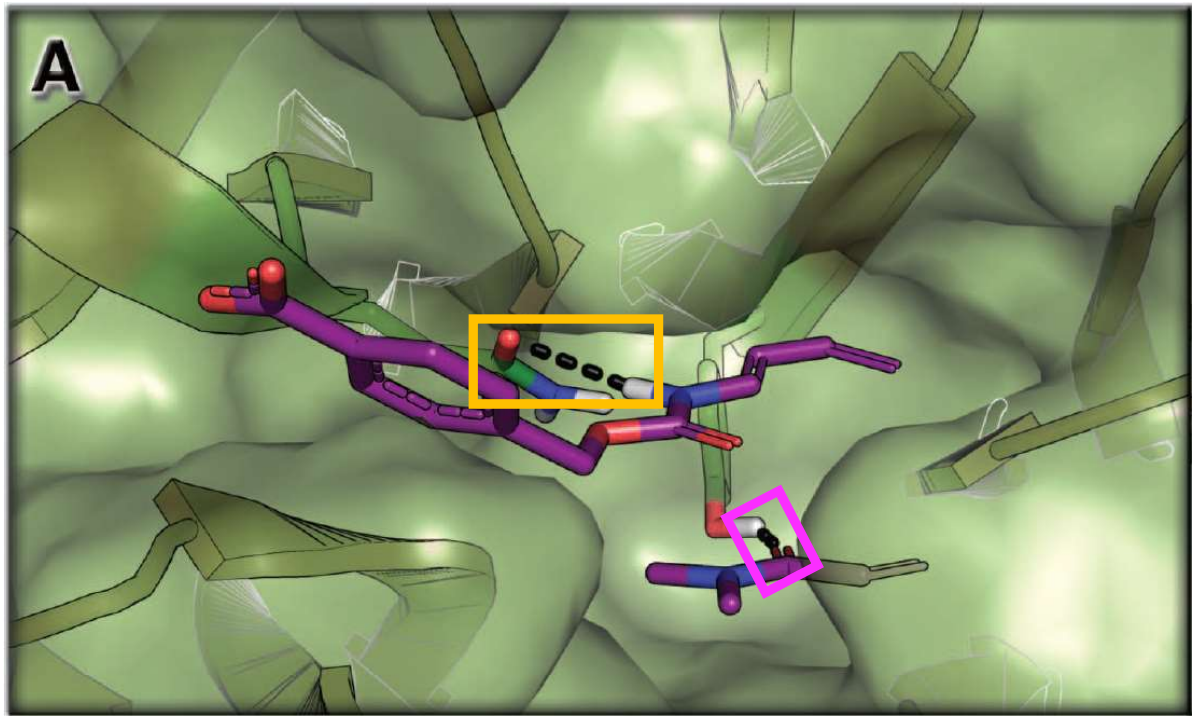

Surface view of the design model (DA_20_00, green) bound to the substrates (diene and dienophile, purple). The frames show the hydrogen bonds designed in **section 2.1.1**.

1. Baker, D. *et al*. *Science* **2010**, *329*, 309.

Appendix. To what extent is TS stabilized by hydrogen bonds?

A. Uncatalyzed

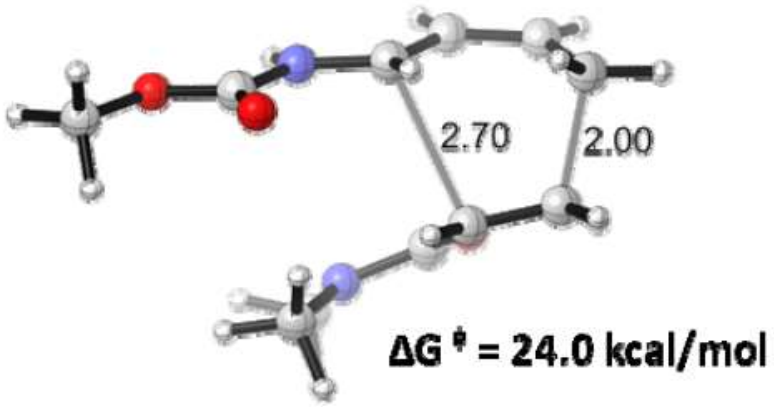

B. Diene-activating residue: Glu; dienophile: Tyr

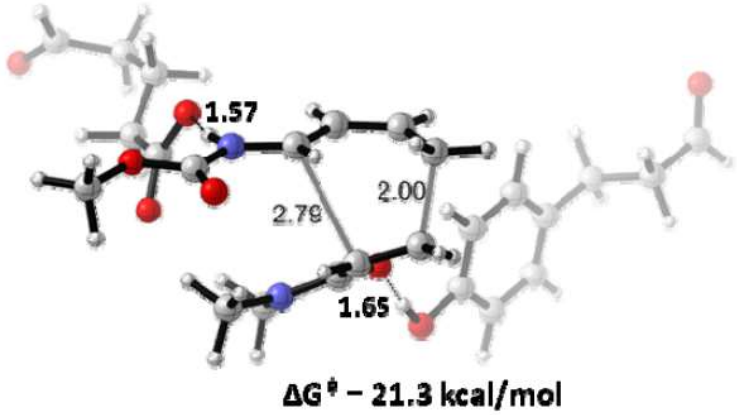

C. Diene-activating residue: Gln; dienophile: Tyr

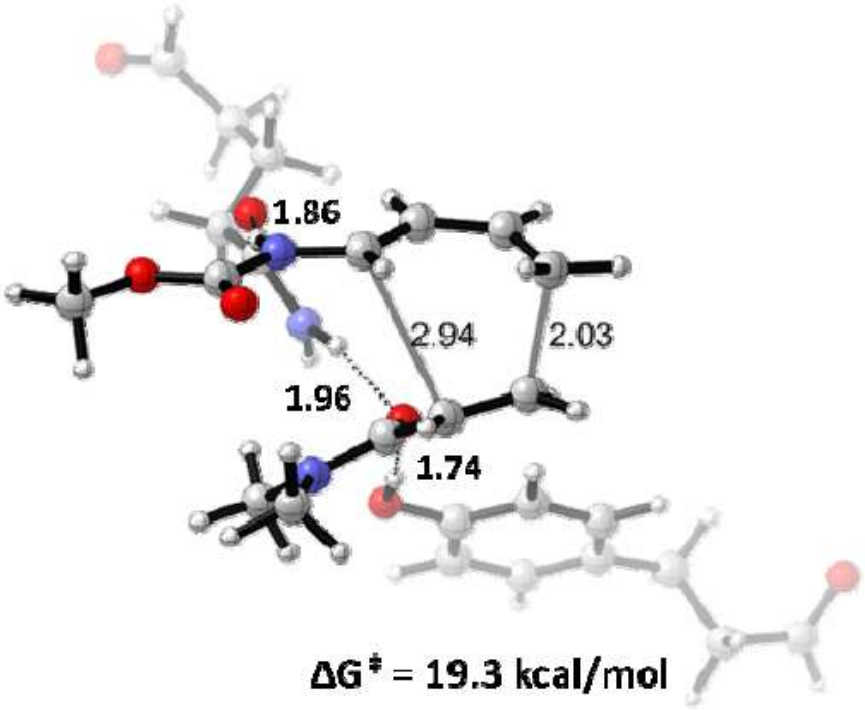

1. Baker, D. *et al*. *Science* **2010**, *329*, 309.

Appendix. How does 10^{19} come?

[1] poses from amide (75,442,752) × [2] poses from hydroxyl (256,608) × [3] numbers of residue positions for 1st catalytic residue (20)

× [4] numbers of residue positions for 2nd catalytic residue (19) × [5] numbers protein scaffold (207) × [6] numbers of TS structures (15)

$= 2.28*10^{19}$

1. Baker, D. *et al*. *Science* **2010**, *329*, 309.

Appendix. How does 10^{19} come?

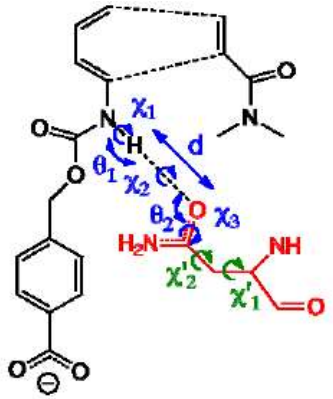

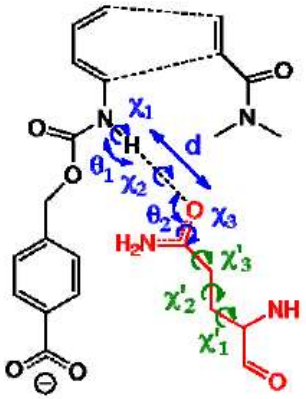

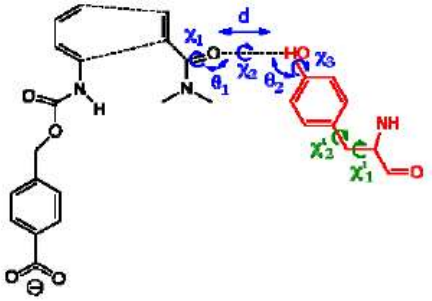

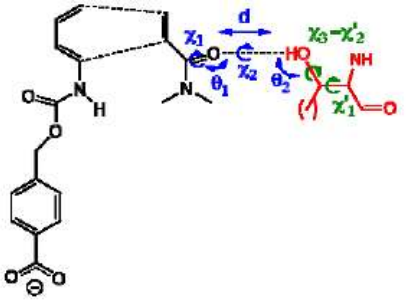

Amino Acid Rotamers

Rotatable Bond	Ideal Value	Deviation	# of Conformations
$\chi 1$	60°/-180°/-60°	+/- 10.0°	21
$\chi 2$	60°/0°/-60°	+/- 20.0°	21
$\chi 3$ (Gln only)	60°/0°/-60°	+/- 20.0°	21
Number of rotamers Asn			441
Number of rotamers Gln			9261

Transition State Orientations

Rotatable Bond	Ideal Value	Deviation	# of Conformations
d	2.0Å	0.1 Å	1
θ1	180.0°	10.0°	1
θ2	120.0°	10.0°	3
$\chi 1$	Free	Every 10°	36
$\chi 2$	Free	Every 10°	36
$\chi 3$	180.0°	+/- 180.0°	2
TS discrete orientations			7776

Total transition state poses off of amide:
(Number of rotamers * Number of orientations) **75442752**

Amino Acid Rotamers

Rotatable Bond	Ideal Value	Deviation	# of Conformations
$\chi 1$	60°/-180°/-60°	+/- 10.0°	9
$\chi 2$ (Tyr only)	0°/90°	+/- 20.0°	9
Number of rotamers Ser			9
Number of rotamers Thr			9
Number of rotamers Tyr			81

Transition State Orientations

Rotatable Bond	Ideal Value	Deviation	# of Conformations
d	2.0Å	0.1 Å	1
θ1	120.0°	10.0°	1
θ2	109.5°	10.0°	1
$\chi 1$	180.0°	+/- 180.0°	2
$\chi 2$	Free	Every 10°	36
$\chi 3$	Free	Every 10°	36
TS discrete orientations			2592

Total transition state poses off of hydroxyl:
(Number of rotamers * Number of orientations) **256608**

1. Baker, D. *et al*. *Science* **2010**, *329*, 309.

Appendix. Active sites of designed Diels Alderases

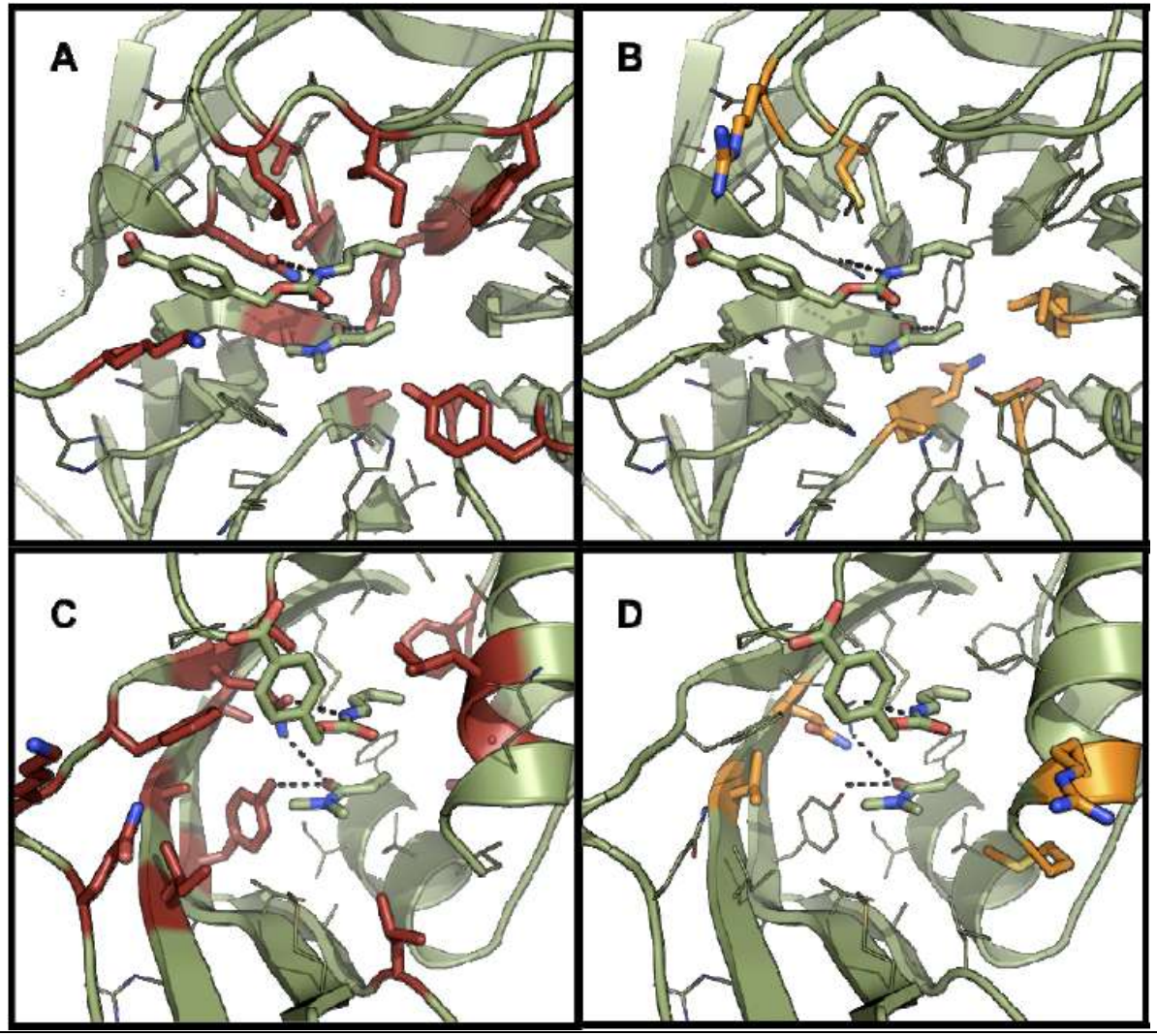

1. Baker, D. *et al*. *Science* **2010**, *329*, 309.

Appendix. Details about the enzyme evaluation in section 3.3

Yields and standard deviations from at least 3 independent experiments obtained for small molecules and protein catalysts in the chromogenic, model hydrazone formation reaction between 4-hydrazino-7-nitro-2,1,3-benzoxadiazole (NBD-H) and 4-nitrobenzaldehyde (4-NBA)

entry	catalyst	[cat] (μM)	yields
1	---	---	6 ± 3
2	aniline	1000	40 ± 4
3	pAF	1000	39 ± 1
4	**LmrR**	10	**46 ± 5**
5	W96A		11 ± 3
6	*bc*PadR1		4 ± 1
7	BSA		5 ± 2
8	**V15pAF**		**72 ± 3**
9	N19pAF		42 ± 2
10	M89pAF		37 ± 2
11	F93pAF		58 ± 1
12	V15K		24 ± 3
13	V15Y		53 ± 1
14	V15pAzF		49 ± 2
15	N19pAzF		38 ± 1
16	M89pAzF		34 ± 1
17	F93pAzF		40 ± 1
18[1]	LmrR*		45
19[1]	V15pAF*		15

after modification in page 21

[1] These yields are for enzymes after their respective modifications with 4-NBA and are the result from a single measurement.

1. Roelfes, G. *et al*. *Nat. Chem.*, 2018, AOP.

Appendix. Comparison of catalytic parameters for LmrR_V15pAF and aniline derivatives

entry	catalyst	rate constant (M^{-2} s^{-1})
1	LmrR_V15pAF	629
2	aniline	1.12
3	anthranilic acid	1.53
4	5-methoxyanthranilic acid	2.07
5	3,5-diaminobenzoic acid	2.71

1. Roelfes, G. *et al*. *Nat. Chem.*, 2018, AOP.

Appendix. Comparison of catalytic parameters for LmrR_V15pAF and other designer enzymes that catalyze bimolecular reactions

entry	enzyme	k_{uncat} (M^{-1} s^{-1})	k_{cat} (s^{-1})	K_{M1} (M)	K_{M2} (M)	k_{cat} / K_{M1} K_{M2} (M^{-2} s^{-1})	EM (M)	1/TS x 10^{-6} (M^{-1})
1	V15pAF	3.95×10^{-4}	5.00×10^{-4}	1.00×10^{-4}	7.92×10^{-3}	6.29×10^{2}	1.27	1.6
2[1]	DA_20_00	1.19×10^{-5}	2.78×10^{-5}	3.50×10^{-3}	1.46×10^{-1}	5.44×10^{-2}	2.33	0.0046
3[1]	DA_42_04	1.19×10^{-5}	8.33×10^{-6}	5.00×10^{-4}	1.62×10^{-2}	1.03×10^{0}	0.70	0.086
4[2]	AB 7D4	1.19×10^{-5}	5.83×10^{-5}	1.00×10^{-3}	1.70×10^{-3}	3.43×10^{1}	4.90	2.87
5[3]	AB 4D5	1.19×10^{-5}	5.83×10^{-5}	1.60×10^{-3}	5.90×10^{-3}	6.18×10^{0}	4.90	0.52
6[4]	Ab 39, A11	1.89×10^{0}	6.70×10^{-1}	1.13×10^{-3}	7.40×10^{-4}	8.01×10^{5}	0.35	0.42
7[5]	Ab 1E9	2.17×10^{-4}	2.17×10^{-1}	2.40×10^{-3}	2.90×10^{-2}	3.11×10^{3}	1000	14.4

1. Roelfes, G. *et al*. *Nat. Chem.*, 2018, AOP.